

# MODULATED HOMOGENEOUS FRICTION: A SEMI-ACTIVE DAMPING STRATEGY

JOSÉ A. INAUDI\*

*University of California at Berkeley and ARCH Ingeniería, Córdoba, Argentina*

## SUMMARY

A control strategy for semi-active friction devices leading to efficient hysteretic dissipaters is proposed. The control algorithm makes the contact force between the sliding surfaces of the damper proportional to the absolute value of the prior local peak of the damper deformation. This control logic leads to a non-linear force–deformation relation that satisfies homogeneity of degree one; this means that, like in a linear viscoelastic damping model, when the deformation is scaled by a constant, the force results are scaled by the same constant. The closed-loop system shows rectangular hysteresis loops which enclose an area proportional to the square of the deformation of the damper. Some characteristics of the dynamic response of structures incorporating this type of semi-active damper are investigated. It is demonstrated that in the case of single-degree-of-freedom models, the period of vibration and decay ratio are independent of the amplitude of vibration. In the case of multi-degree-of-freedom models with this type of nonlinearity, the free-vibration response can exhibit natural modes of vibration. A linearization method is proposed and modelling tools for the delay associated with actuator dynamics and for the flexibility of the brace connecting the damper to the structure are presented.

KEY WORDS: damping; active control; friction; semi-active control; hysteretic damping

## 1. INTRODUCTION

Variable-resistance dissipaters, also referred to as semi-active dampers in the literature, have been proposed as cost-efficient vibration-control systems for flexible structures. Semi-active viscous dampers and semi-active friction dampers have been utilized in suspension systems of automobiles<sup>1–3</sup> and recently proposed for building structures or bridges subjected to earthquake excitation.<sup>4–13</sup>

Both variable viscous dampers and variable friction dampers can modulate the rate of energy dissipation by real-time adjustment of the damper resistance to deformation.<sup>2</sup> Consider, for example, a variable viscous damper satisfying

$$f(t) = c(t) \frac{d\Delta}{dt}(t) \quad (1)$$

where  $c(t)$  is the controllable damping constant (positive) and  $\Delta(t)$  is the damper deformation. The energy dissipation rate is

$$\frac{dE}{dt} = c(t) \left( \frac{d\Delta}{dt}(t) \right)^2 \geq 0 \quad (2)$$

where  $E(t)$  is the energy dissipated in the damper up to time  $t$ . As indicated in equation (1), by controlling  $c(t)$ , the force in the damper can be controlled subject to the constraint in equation (2), and the damper can be

---

\*Research Engineer at University of California and Engineering Consultant at ARCH Ingeniería, Argentina.

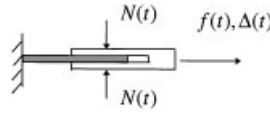


Figure 1. Schematic description of a semi-active friction dissipater

utilized as an actuator or force generator to provide some of the benefits of fully active control systems but with much reduced cost and complexity because very little power is required to operate the variable damper.<sup>3</sup>

A semi-active friction damper (Figure 1) consists of two bodies which slide with respect to each other subjected to a controllable contact force  $N(t)$ , generating a dissipative force proportional to the contact force  $N(t)$  ( $\geq 0$ ) and the coefficient of friction  $\mu$  between the surfaces. The damper force is then

$$\begin{aligned} f(t) &= \mu N(t) \operatorname{sgn}\left(\frac{d\Delta(t)}{dt}\right) \quad \text{if } \frac{d\Delta}{dt}(t) \neq 0 \\ -\mu N(t) &\leq f(t) \leq \mu N(t) \quad \text{if } \frac{d\Delta}{dt}(t) = 0 \end{aligned} \quad (3)$$

The rate of energy dissipation in this dissipater is

$$\frac{dE}{dt} = N(t)\mu \left| \frac{d\Delta}{dt}(t) \right| \geq 0 \quad (4)$$

which is non-negative for any  $N(t) \geq 0$ .

Different control strategies can be implemented to improve the dynamical behaviour of structures utilizing semi-active dampers.<sup>14</sup> Stability of the closed-loop system is not compromised by any controller because the forces generated by a semi-active viscous damper or by a semi-active friction damper are always dissipative.

Because the slip force  $\mu N$  is constant in a passive Coulomb friction damper, this damper sticks without dissipating energy in the case of low-level excitation and dissipates energy proportionally to the first power of the amplitude of deformation only when slippage is induced by sufficiently high excitation levels. To improve the energy dissipation process of a friction damper it seems natural to increase the slip force with increasing damper deformation by increasing the contact force through feedback of damper deformation.

Following this concept, several control algorithms have been proposed. Akbay and Aktan<sup>5</sup> have proposed a control scheme by which the slip force is adjusted actively to allow slippage in controlled amounts during the response of the structure. Another operational algorithm proposed for the semi-active friction damper consists of changes in the slip force with prespecified increments at fixed-time intervals such that the slip force is lowered if slippage does not take place in the previous decision interval, and raised if the device slips in the previous decision interval.<sup>4, 15, 13</sup> Dowdell and Cherry<sup>6</sup> have proposed a clamp-and-release scheme or off-on control for cases in which the slip force can take two values, or a variable slip force control in which the slip load is proportional to the deformation of the damper and connecting brace. In bridge applications, Yang and Lu<sup>12</sup> have proposed a multi-stage slip-force control scheme in which the slip force is changed when the deformation of the structure exceeds specified thresholds.

In this work, a new control scheme leading to a semi-active frictional device with resistance proportional to the element deformation is proposed and investigated. The dynamical response of single-degree-of-freedom (SDOF) and multi-degree-of-freedom (MDOF) structures with this semi-active dissipaters is analysed and a linearization technique for the analysis of structures with semi-active friction dampers operated according to the proposed control logic is applied.

## 2. PROPOSED CONTROL LOGIC

The proposed control algorithm is a collocated dynamic feedback law which uses the deformation of the damper as the only feedback signal to define the contact force  $N(t)$  of the semi-active friction damper.

Mathematically, the controller is expressed as

$$N(t) = g|P[\Delta(t)]| \quad (5)$$

where  $g$  is the positive gain coefficient with units of stiffness and  $P[\Delta(t)]$  the operator defined as follows:

$$P[\Delta(t)] = \Delta(t - s) \quad \text{where } s = \left\{ \min x \geq 0: \frac{d\Delta}{dt}(t - x) = 0 \right\} \quad (6)$$

and such that  $\Delta(t - s)$  is a local peak of the deformation signal.

Because the output of  $P[\Delta(t)]$  is equal to the value of the input signal at the prior closest local peak,  $P[\Delta(t)]$  is referred to as prior-local-peak operator herein.

In equation (5),  $|P[\Delta(t)]|$  makes the contact force  $N(t)$  proportional to the deformation signal. However, the controller has memory because the past of the deformation signal is required to determine the control signal  $N(t)$  at current time  $t$ . The absolute value in this expression ensures a non-negative value for the contact force.

The output of the prior-local-peak operator is illustrated in Figure 2 for an arbitrary deformation signal;  $\Delta(t)$  is shown in thin line and  $P[\Delta(t)]$  is the piecewise constant signal shown in thick line in the figure. It is not difficult to prove that the prior-local-peak operator satisfies the property of homogeneity of degree one (HD1), i.e.  $P[\beta\Delta(t)] = \beta P[\Delta(t)]$  for any  $\beta \in \mathfrak{R}$ .

When operated with the proposed control law (equation (5)), the force in the semi-active damper is given by

$$\begin{aligned} f[\Delta(t)] &= g\mu|P[\Delta(t)]|\text{sgn}\left(\frac{d\Delta(t)}{dt}\right) \quad \text{if } \frac{d\Delta}{dt}(t) \neq 0 \\ -g\mu|P[\Delta(t)]| &\leq f[\Delta(t)] \leq g\mu|P[\Delta(t)]| \quad \text{if } \frac{d\Delta}{dt}(t) = 0 \end{aligned} \quad (7)$$

We call this closed-loop system: modulated homogeneous friction (MHF). Figure 3 shows the hysteresis loops of a MHF dissipater for the deformation signal shown in Figure 2. Rectangular hysteresis loops with variable slip force can be observed in Figure 3 where the force of the MHF dissipater has been normalized as  $f[\Delta(t)]/(g\mu)$ .

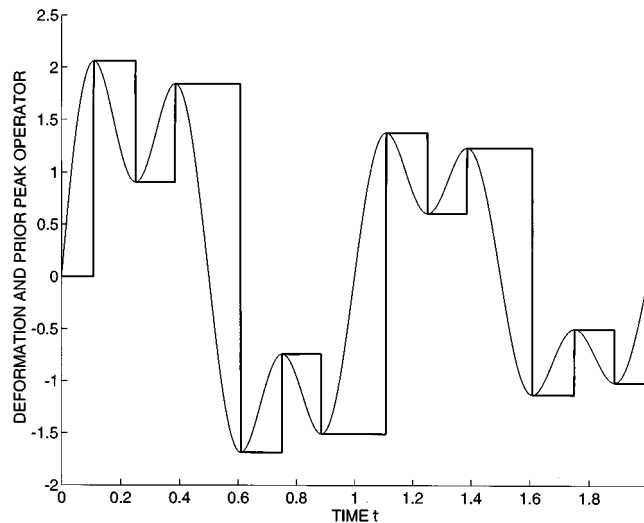


Figure 2. Prior-local-peak operator  $P[\Delta(t)]$  (thick line) for arbitrary deformation signal  $\Delta(t)$  (thin line)

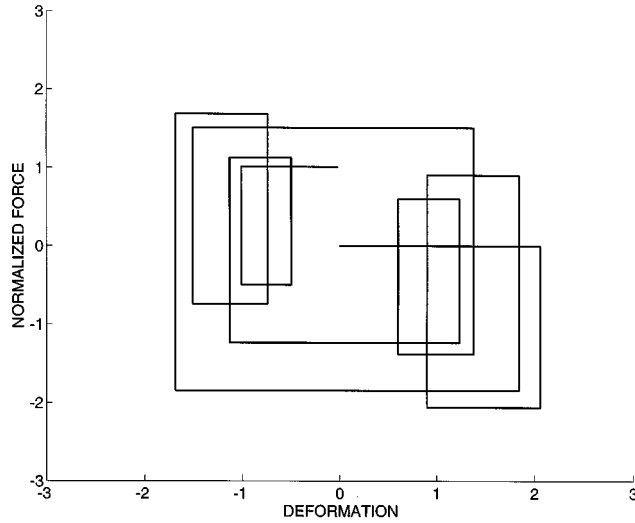


Figure 3. Hysteresis loops of a MHF dissipater. Deformation  $\Delta(t)$  in horizontal axis and normalized force  $f[\Delta(t)]/(\mu g)$  in vertical axis

Equation (7) is an HD1 force–deformation relation, because

$$f[\beta\Delta(t)] = g\mu|P[\beta\Delta(t)]|\operatorname{sgn}\left(\beta\frac{d\Delta(t)}{dt}\right) \quad (8)$$

which for  $\beta > 0$  gives

$$f[\beta\Delta(t)] = g\mu\beta|P[\Delta(t)]|\operatorname{sgn}\left(\frac{d\Delta(t)}{dt}\right) = \beta f[\Delta(t)] \quad (9)$$

while for  $\beta < 0$  yields

$$f[\beta\Delta(t)] = g\mu|\beta||P[\Delta(t)]|(-\operatorname{sgn}\left(\frac{d\Delta(t)}{dt}\right)) = \beta f[\Delta(t)] \quad (10)$$

The MHF system (equation (7)) yields a rate-independent force–deformation relation such that the following similarity property holds:

$$f[\Delta(\beta t)] = z(\beta t) \quad \text{with } z(t) = f[\Delta(t)] \quad (11)$$

The implication of this property is that the dissipater dissipates the same amount of energy in a sinusoidal deformation cycle of any frequency.

In the case of sinusoidal deformation of amplitude  $\Delta_0$ , the hysteresis loop of MHF is rectangular as shown in Figure 4. In contrast with passive Coulomb friction in which the dissipation of energy is proportional to the first power of the deformation amplitude because the slip force is fixed in this dissipater, the energy dissipation per cycle  $E_d$  in a MHF dissipater is

$$E_d = 4g\mu\Delta_0^2 \quad (12)$$

This expression can be matched for any deformation amplitude to the dissipation of energy of a linear hysteretic element (or structural damping model), which in the frequency domain is expressed as

$$F(\omega) = jS_h \operatorname{sgn}(\omega)\Delta(\omega) \quad (13)$$

where  $F(\omega)$  is the Fourier transform of the force signal,  $\Delta(\omega)$  is the Fourier transform of the deformation signal,  $j = \sqrt{-1}$ , and  $S_h$  is the parameter with stiffness units characterizing the damping model. The energy

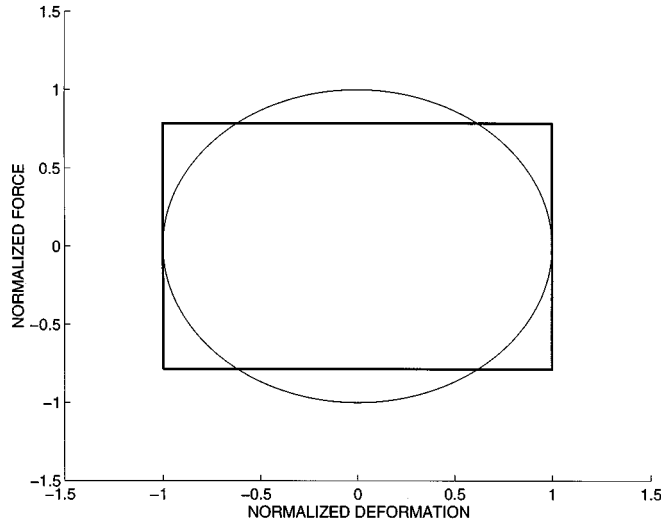


Figure 4. Hysteresis loop of a MHF dissipater subjected to sinusoidal deformation (thick line) and hysteresis loop of an equivalent linear hysteretic element (thin line)

dissipation in a cycle of harmonic deformation of this linear model is

$$E_d = \pi S_h \Delta_0^2 \quad (14)$$

Therefore, both models dissipate the same amount of energy in a sinusoidal deformation cycle if

$$S_h = \frac{4g\mu}{\pi} \quad (15)$$

It can be proven that the linear model in equation (13) with  $S_h$  satisfying equation (15) is the equivalent linear element for MHF (equation (7)) resulting from the use of the harmonic linearization technique.<sup>14</sup> In this method, an equivalent linear model is sought by minimizing the square of the difference between the force of the non-linear model and that of the equivalent linear model over a cycle of sinusoidal deformation.

Figure 4 shows the hysteresis loops of the MHF element (in thick line) and that of an equivalent linear hysteretic element (thin line) corresponding to a cycle of sinusoidal deformation  $\Delta(t) = \Delta_0 \sin \omega t$ . The normalized forces  $f(t)/S_h$  of both MHF and linear hysteretic damping are plotted as functions of the normalized deformation  $\Delta(t)/\Delta_0$ . The constant  $S_h$  satisfies equation (15); therefore, both hysteresis loops in this figure enclose the same area for any deformation amplitude. The model in equation (13) with  $S_h$  satisfying equation (15) can be utilized as an equivalent linear element for MHF; this linearization will be used later to estimate the response of SDOF and MDOF structures with MHF.

The proposed control logic that makes the prior-local-peak operator yields a more efficient dissipater than a control logic that makes the contact force simply proportional to the current deformation signal. Assume the following memoryless feedback law is utilized for the semi-active friction damper

$$N(t) = e|\Delta(t)| \quad (16)$$

where  $e$  is the constant feedback gain with units of stiffness. This control scheme leads also to a homogeneous force–deformation relation because from equations (3) and (16)

$$f\left(\Delta(t), \frac{d\Delta(t)}{dt}\right) = e\mu|\Delta(t)| \operatorname{sgn}\left(\frac{d\Delta(t)}{dt}\right) = e\mu\Delta(t) \operatorname{sgn}\left(\Delta(t) \frac{d\Delta(t)}{dt}\right) \quad (17)$$

which is an HD1 variable-stiffness element referred to as Reid's model of hysteretic damping.<sup>16,17</sup> This model yields triangular hysteresis loops enclosing only half the area enclosed by the rectangular hysteresis of the proposed closed-loop system for the same value of maximum force, making this control scheme (equation (16)) less efficient than MHF (equation (5)).

### 3. SDOF STRUCTURAL MODELS INCORPORATING MHF DISSIPATERS

#### 3.1. Free vibration of SDOF structures with MHF

Consider the following model of a SDOF structure with a semi-active friction damper operated according to the proposed control law (equation (7)):

$$m \frac{d^2 y}{dt^2}(t) + \omega^2 m y(t) + g \mu |P[y(t)]| \operatorname{sgn} \left( \frac{dy}{dt}(t) \right) = 0 \quad (18)$$

where  $m$  is the mass of the oscillator,  $\omega$  the undamped natural frequency and  $y(t)$  the displacement. Since each term in this differential equation is HD1, the oscillator is HD1.<sup>14</sup> The free vibration response for initial conditions  $y(0) = Y_n$  and  $dy/dt(0) = 0$  is periodic with a decay ratio independent of the amplitude of vibration as we demonstrate in the following.

For an oscillatory response, it is required that

$$\alpha = \frac{g \mu}{\omega^2 m} < \frac{1}{2} \quad (19)$$

It can be demonstrated that for  $\alpha \geq \frac{1}{2}$ , the displacement  $y(t)$  does not exhibit an oscillatory response in the absence of external loading.

During the first half cycle,  $P[y(t)] = y(0) = Y_n$  and the solution of equation (18) can be obtained as

$$y(t) = \alpha Y_n + Y_n(1 - \alpha) \cos \omega t, \quad 0 \leq t \leq \pi/\omega \quad (20)$$

At  $t = \pi/\omega$ , the displacement reaches a local peak

$$y\left(\frac{\pi}{\omega}\right) = (2\alpha - 1) Y_n \quad (21)$$

For  $\pi/\omega < t \leq 2\pi/\omega$ ,  $P[y(t)] = (2\alpha - 1) Y_n$  and the solution can be obtained in a similar fashion. After one cycle,

$$y\left(\frac{2\pi}{\omega}\right) = Y_{n+1} = (1 - 2\alpha)^2 Y_n \quad (22)$$

Therefore, the period of oscillation and decay ratio are

$$T = \frac{2\pi}{\omega} \quad (23)$$

$$\gamma = \frac{Y_{n+1}}{Y_n} = (1 - 2\alpha)^2 \quad (24)$$

This means that provided  $\alpha < \frac{1}{2}$ , the period of vibration of this non-linear system is unchanged by the feedback gain  $g$  of the semi-active friction dissipater while the decay ratio is highly dependent on  $g$  (see equations (24) and (19)).

Figure 5 shows the displacement of the oscillator for various values of  $\alpha$  and  $\omega = 2\pi$  rad/s during free vibration. As it observed in the figure, MHF can increase the damping of a structure without modifying its vibration frequencies.

An equivalent damping ratio  $\xi_e$  can be defined for this oscillator by equating the decay ratio in equation (24) with the decay ratio  $e^{-2\pi\xi_e/\sqrt{1-\xi_e^2}}$  of a linear oscillator with natural frequency  $\omega$  and damping ratio  $\xi_e$ ,

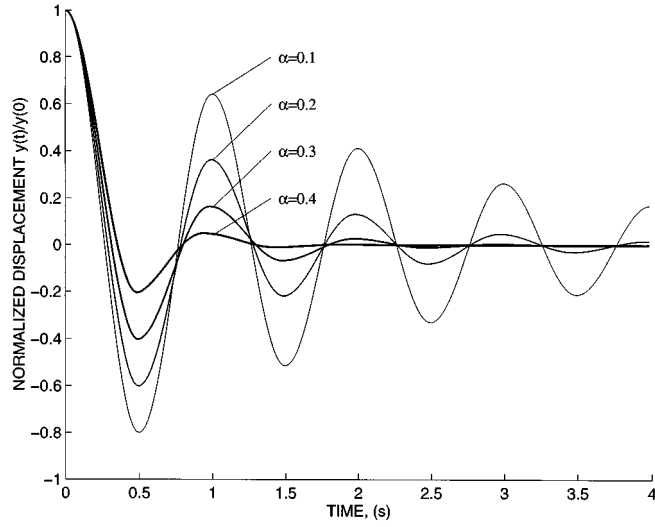


Figure 5. Free vibration response of SDOF oscillator with MHF

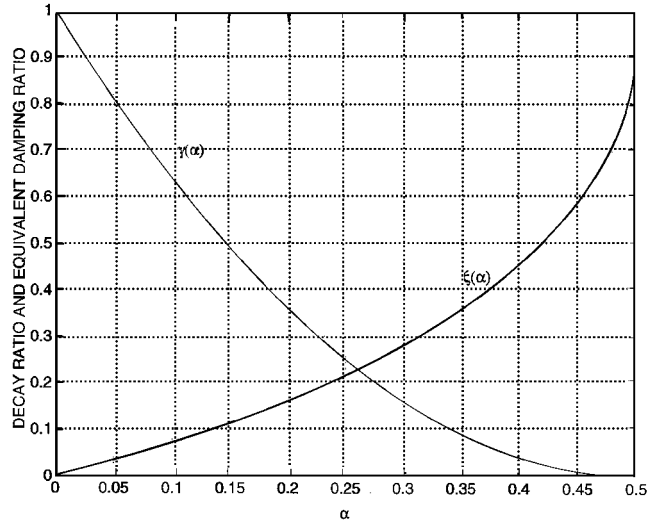


Figure 6. Decay ratio and equivalent damping ratio of a SDOF oscillator with MHF in free in free vibration

which yields

$$\zeta_e = \frac{-\ln(\gamma)}{\sqrt{4\pi^2 + \ln^2 \gamma}} \quad (25)$$

where  $\gamma$  is given in equation (24). The functions  $\gamma(\alpha)$  and  $\zeta_e(\alpha)$  are plotted in Figure 6. This figure can be used to estimate the apparent damping constant of SDOF structures as a function of the gain of the MHF controller.

### 3.2. Response to harmonic excitation

Let us compute the steady-state response of the SDOF oscillator with MHF subjected to sinusoidal excitation. The equation of motion to be solved is

$$\frac{d^2 y}{dt^2}(t) + \omega^2 y(t) = -\alpha \omega^2 |P[y(t)]| \operatorname{sgn}\left(\frac{dy}{dt}(t)\right) + W \sin(\varpi t + \varphi) \quad (26a)$$

$$y(-\infty) = 0, \quad \frac{dy(-\infty)}{dt} = 0 \quad (26b)$$

where  $W$  is the amplitude of the excitation signal (acceleration units),  $\varpi$  the forcing frequency and  $\varphi$  the unknown phase included so that at steady-state response,

$$y(0) = Y \quad \text{and} \quad \frac{dy}{dt}(0) = 0 \quad (27)$$

where  $Y$  is the amplitude of the displacement response at steady state.  $Y$  and  $\varphi$  are unknown and can be computed as follows.

For the first half cycle of the steady-state response,  $P[y(t)] = Y$  and for  $\varpi \neq \omega$ ,

$$y(t) = \alpha Y + \frac{W}{\omega^2 - \varpi^2} \sin(\varpi t + \varphi) + B \sin \omega t + C \cos \omega t, \quad 0 \leq t \leq \pi/\varpi \quad (28)$$

where the constants of integration  $B$  and  $C$  are

$$B = -\frac{W\varpi}{\omega(\omega^2 - \varpi^2)} \cos \varphi, \quad C = Y(1 - \alpha) - \frac{W}{\omega^2 - \varpi^2} \sin \varphi \quad (29)$$

At  $t = \pi/\varpi$ ,

$$y\left(\frac{\pi}{\varpi}\right) = -Y \quad \text{and} \quad \frac{dy}{dt}\left(\frac{\pi}{\varpi}\right) = 0 \quad (30)$$

Therefore, from equations (28) and (30), we obtain two non-linear equations in  $Y$  and  $\varphi$  whose solution gives us the steady-state response of the oscillator. These are

$$Y(1 + \alpha) + \frac{W}{\omega^2 - \varpi^2} \sin(\pi + \varphi) + B \sin\left(\frac{\omega\pi}{\varpi}\right) + C \cos\left(\frac{\omega\pi}{\varpi}\right) = 0 \quad (31a)$$

$$\frac{W\varpi}{\omega^2 - \varpi^2} \cos(\pi + \varphi) + B\omega \cos\left(\frac{\omega\pi}{\varpi}\right) - C\omega \sin\left(\frac{\omega\pi}{\varpi}\right) = 0 \quad (31b)$$

Figure 7 shows with ‘o’ symbols the normalized amplitude  $|Y\omega^2/W|$  of this oscillator subjected to a sinusoidal excitation signal as a function of the forcing frequency  $\varpi$  for various values of  $\alpha$  and  $\omega = 2\pi$  rad/s. The figure also shows (in solid line) the amplitude of the response of the equivalent linear oscillator which in the frequency domain satisfies

$$[-\varpi^2 + \omega^2 + j \frac{S_h}{m} \operatorname{sgn}(\varpi)] Y(\varpi) = W(\varpi) \quad (32)$$

where  $Y(\varpi)$  is the Fourier transform of  $y(t)$ ,  $W(\varpi)$  the Fourier transform of the excitation, and  $S_h$  is the parameter of the equivalent linear model given in equation (15). From equations (15), (19) and (32), we obtain

$$\left| \frac{Y\omega^2}{W} \right| = \frac{\omega^2}{\sqrt{(\omega^2 - \varpi^2)^2 + ((4\alpha\omega^2/\pi) \operatorname{sgn}(\varpi))^2}} \quad (33)$$

which gives the normalized steady-state amplitude of the equivalent linear hysteretic oscillator. This function is plotted in solid line in Figure 7 which shows very good accuracy of the linearization method.

To analyse the vibration reduction achievable with MHF, the response of a SDOF oscillator with undamped period of vibration  $T = 1$  s and various values of  $\alpha$  subjected to the El Centro ground-acceleration



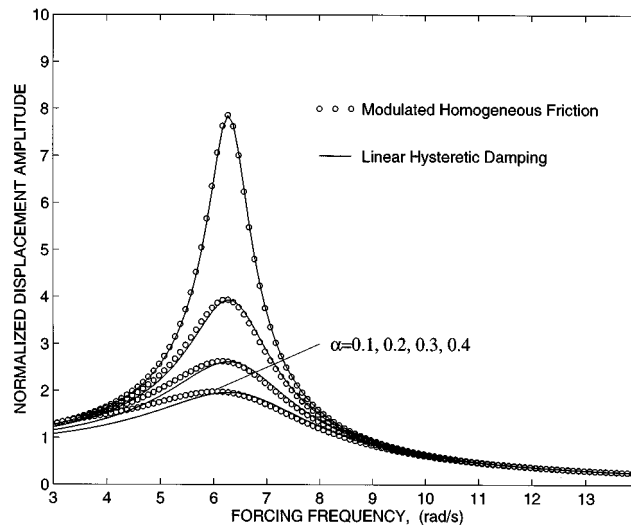


Figure 7. Comparison of the frequency response of a SDOF oscillator with MHF with that of an equivalent linear SDOF system

Table I. Maximum displacement and maximum acceleration of SDOF structure ( $\omega = 2\pi$  rad/s) with MHF subjected to the El Centro earthquake (1940)

$\alpha$	Maximum displacement (cm)	Maximum acceleration ( $\text{cm/s}^2$ )
0	20.6	814
0.05	15.6	637
0.15	9.4	415
0.30	6.9	337
0.40	5.7	293
0.50	5.4	263

Table II. Maximum displacement and maximum acceleration of equivalent linear SDOF ( $\omega = 2\pi$  rad/s) structure subjected to the El Centro earthquake (1940)

$\alpha$	Equivalent damping ratio $\xi_e(\alpha)$	Maximum displacement (cm)	Maximum acceleration ( $\text{cm/s}^2$ )
0	0.00	20.6	814
0.05	0.032	15.1	594
0.15	0.096	8.9	363
0.30	0.191	5.9	249
0.40	0.255	4.9	218
0.50	0.318	4.1	211

signal (Imperial Valley, 1940) was computed. The maximum deformation and acceleration obtained are shown in Table I. The beneficial effect of energy-dissipation increase by MHF can be appreciated in the table.

Table II shows the deformation and acceleration estimates obtained using an equivalent linear SDOF oscillator with natural period  $T = 1$  s and equivalent damping ratio

$$\xi_e = \frac{4\alpha}{2\pi} \quad (34)$$

which is obtained applying the modal strain energy method to this oscillator.<sup>18</sup> Comparing Tables I and II, it can be observed that the accuracy of this linearization technique worsens as  $\alpha$  increases.

#### 4. MDOF STRUCTURAL MODELS INCORPORATING MHF DISSIPATERS

##### 4.1. Modes of vibration

A structural system with semi-active friction dampers can show modes of vibration during free vibration if certain conditions are satisfied. This characteristic is shared by a number of HD1 dynamical systems.<sup>14</sup>

Consider the following model of an  $N$ -DOF structure:

$$M \frac{d^2 y}{dt^2}(t) + Ky(t) + \sum_{i=1}^{N_e} L_i^T f_i[\Delta_i(t)] = 0 \quad (35)$$

where  $M$  is the mass matrix,  $K$  the stiffness matrix,  $y(t)$  the displacement vector,  $N_e$  the number of friction dissipaters,  $L_i$  the transformation from structure displacements to the deformation of the  $i$ th friction damper

$$\Delta_i(t) = L_i y(t) \quad (36)$$

and  $f_i[\Delta_i(t)]$  is the force in the  $i$ th MHF dissipater:

$$f_i[\Delta_i(t)] = \mu g_i |P[L_i y(t)]| \operatorname{sgn} \left( L_i \frac{dy}{dt}(t) \right) \quad (37)$$

We have assumed the same coefficient of friction  $\mu$  for all dissipaters, and a feedback gain  $g_i$  for the  $i$ th dissipater. It is worth emphasizing that each dissipater is operated by an independent controller using the deformation of each dissipater as feedback signal.

Let the response be parallel to a mode of vibration  $\phi_l$  of the undamped structure,

$$y(t) = \phi_l q_l(t) \quad (38)$$

where  $q_l(t)$  is the modal co-ordinate. If equation (38) is satisfied,

$$f_i(t) = \mu g_i |L_i \phi_l| P[q_l(t)] \operatorname{sgn}(L_i \phi_l) \operatorname{sgn} \left( \frac{dq_l}{dt}(t) \right) = \mu g_i L_i \phi_l |P[q_l(t)]| \operatorname{sgn} \left( \frac{dq_l}{dt}(t) \right) \quad (39)$$

If we define

$$D = \mu \sum_{i=1}^{N_e} L_i^T g_i L_i \quad (40)$$

from equations (35) and (38) we can write

$$M \phi_l \frac{d^2 q_l}{dt^2}(t) + K \phi_l q_l(t) + D \phi_l P[q_l(t)] \operatorname{sgn} \left( \frac{dq_l}{dt}(t) \right) = 0 \quad (41)$$

If  $D$  is classical, the vectors  $M \phi_l$ ,  $K \phi_l$  and  $D \phi_l$  are parallel for all  $\phi_l$ ,  $l = 1, 2, \dots, N$  and the system can show modes of vibration if the initial condition is parallel to a particular mode shape. Furthermore, the modal co-ordinate satisfies in this case

$$\frac{d^2 q_l}{dt^2}(t) + \omega_l^2 q_l(t) + \alpha_l \omega_l^2 P[q_l(t)] \operatorname{sgn} \left( \frac{dq_l}{dt}(t) \right) = 0 \quad (42)$$

where

$$\omega_l^2 M \phi_l = K \phi_l, \quad \alpha_l = \frac{\phi_l^T D \phi_l}{\omega_l^2 \phi_l^T M \phi_l} \quad (43)$$

Equation (42) corresponds to the equation of motion of a SDOF model with MHF already analysed in Section 3.

#### 4.2. Linearization of MDOF structures including MHF

Consider the following MDOF model of a structure with MHF dissipaters:

$$M \frac{d^2 y}{dt^2}(t) + Ky(t) + \sum_{i=1}^{N_e} L_i^T f_i[\Delta_i(t)] = L_w w(t) \quad (44)$$

where  $L_w$  is the excitation influence vector and  $w(t)$  the excitation signal. Although the response of this system to arbitrary excitation can be computed using step-by-step numerical integration methods, the fact that this is an HD1 dynamical system allows for very accurate linearization.<sup>14</sup> In this case, the linearization of the MHF elements is done using linear hysteretic elements as described in equations (13) and (15). Therefore, the equivalent linear system can be expressed in the frequency domain as

$$[-\omega^2 M + K + j \operatorname{sgn}(\omega) S] Y(\omega) = L_w W(\omega) \quad (45)$$

where  $Y(\omega)$  is the Fourier transform of the displacement vector,  $W(\omega)$  the Fourier transform of the excitation signal  $w(t)$  and

$$S = \frac{4\mu}{\pi} \sum_{i=1}^{N_e} L_i^T g_i L_i \quad (46)$$

This expression has been obtained by assembling the equivalent linear elements of each dissipater (see equation (15)).

To show the efficacy of MHF in reducing vibrations of MDOF models and to demonstrate the accuracy of the proposed linearization technique, the response of a six-storey steel-frame structure with MHF dissipaters connected through diagonal braces and subjected to seismic motion is computed. The frame utilized in this numerical example is shown in Figure 8. For simplicity, the lateral displacements  $y_i(t)$   $i = 1, 2, \dots, 6$  of each floor are taken as the degrees of freedom of the dynamical problem. The floor masses are lumped in the diagonal elements of the mass matrix of the frame:

$$M = \operatorname{diag}(2.527, 2.527, 2.527, 2.527, 2.527, 2.527) \text{ kNs}^2/\text{cm} \quad (47)$$

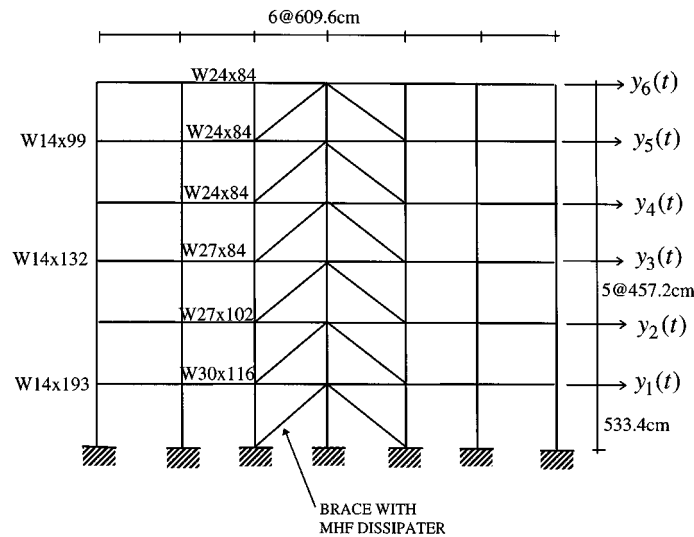


Figure 8. Moment-resistant steel frame used for numerical example of MDOF structures incorporating MHF

The stiffness matrix of the frame is computed as

$$K = \begin{bmatrix} 3.223 & -2.334 & 0.3078 & -0.0316 & 0.0030 & 0.0017 \\ & 3.655 & -1.777 & 0.2628 & -0.0254 & 0.0027 \\ & & 2.892 & -1.605 & 0.2226 & -0.0209 \\ & & & 2.454 & -1.263 & 0.1798 \\ & \text{symm.} & & & 2.045 & -0.9818 \\ & & & & & 0.8178 \end{bmatrix} 10^3 \text{ kN/cm} \quad (48)$$

The inherent damping of the structure without the dissipaters was modelled as a classical damping matrix with model damping ratios of 0.5 per cent. Twelve MHF dissipaters connecting adjacent floors through diagonal braces were incorporated in the model. The friction coefficient of the semi-active friction dampers was taken as  $\mu = 0.20$ , and the feedback gains  $g_l$ ,  $l = 1, \dots, 12$  of the MHF dampers were assumed identical for simplicity.

Three cases with different feedback gains in the MHF dissipaters were considered:  $g_l = 0$  in Case I (bare frame);  $g_l = 98.1 \text{ kN/cm}$  in Case II and  $g_l = 490.5 \text{ kN/cm}$  in Case III.

The response of the frame subjected to the north-south component of the El Centro earthquake (Imperial Valley, 1940) was computed for Cases I–III using numerical simulation. The efficiency of MHF dissipaters in reducing deformations of the frame can be observed in Figure 9 where the roof displacement  $y_6(t)$  is plotted for the structure without MHF dissipaters (Case I), and with MHF dissipaters (Cases II and III). The maximum forces required in the MHF dissipaters for this simulation were  $f_{\max} = 49.9 \text{ kN}$  in Case II and  $f_{\max} = 194.7 \text{ kN}$  in Case III. The maximum deformations in the first storey were 5.24 cm (Case I), 3.12 cm (Case II), and 2.70 cm (Case III).

To demonstrate the excellent accuracy achieved using the proposed linearization technique for the estimation of the response of MDOF structures with MHF dissipaters, the response of the frame in Case III was estimated by linearizing the MHF dissipaters. The matrix  $S$  (equation (46)) was computed for

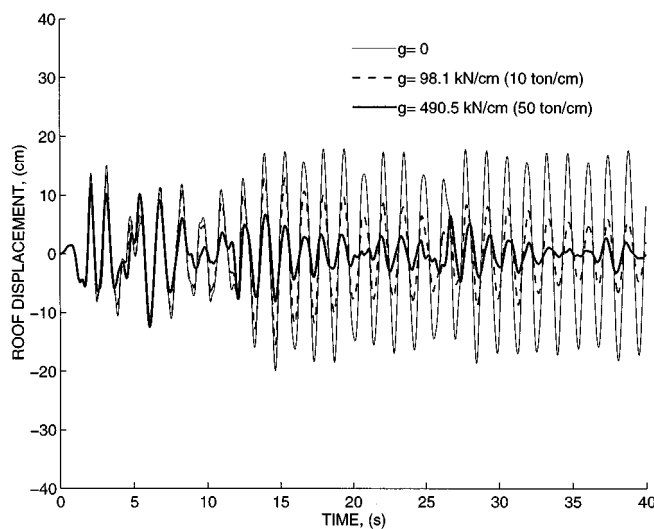


Figure 9. Efficiency of MHF in reducing structure deformations

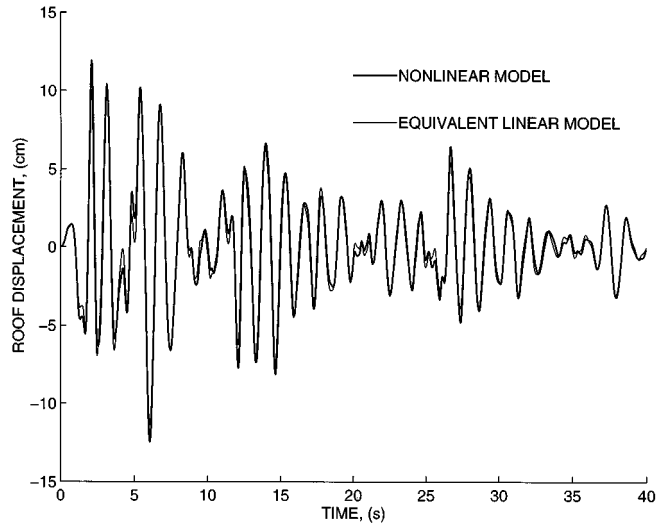


Figure 10. Comparison of exact response of frame (Case III) with estimate obtained using the proposed linearization technique

this case as

$$S = \begin{bmatrix} 292.5 & -157.65 & 0 & 0 & 0 & 0 \\ & 315.3 & -157.65 & 0 & 0 & 0 \\ & & 315.3 & -157.65 & 0 & 0 \\ & & & 315.3 & -157.65 & 0 \\ \text{symm} & & & & 315.3 & -157.65 \\ & & & & & 157.65 \end{bmatrix} \text{ kN/cm} \quad (49)$$

The response of the equivalent linear model was then obtained using fast Fourier transform. Figure 10 compares the roof displacement of the frame with MHF dissipaters for Case III (non-linear model) with the corresponding estimate obtained using the equivalent linear model. Excellent accuracy is obtained with the proposed linearization method. It is worth mentioning that the accuracy obtained is independent of the excitation level because both the non-linear model and the equivalent linear model are HD1.

##### 5. MHF DISSIPATER INCLUDING ACTUATOR DYNAMICS

The implementation of the proposed control algorithm requires hardware capable of applying the variable contact force  $N(t)$ . This procedure cannot be done instantaneously; therefore, there will always be a delay between the detection of a local peak in the deformation signal and the application of the desired contact force. Let us model the reaction time of the actuating mechanism with a first-order model:

$$\frac{dN}{dt}(t) = -\frac{1}{\tau_N} N(t) + \frac{g}{\tau_N} |P[\Delta(t)]|, \quad N(0) = N_0 \quad (50)$$

where  $\tau_N$  is the time constant of the actuating mechanism defining the speed of the actuator. For  $P[\Delta(t)] = p = \text{constant}$ , the steady-state response of equation (50) is

$$N_{ss} = g|p| \quad (51)$$

which coincides with the control contact force provided by the model in equation (5).

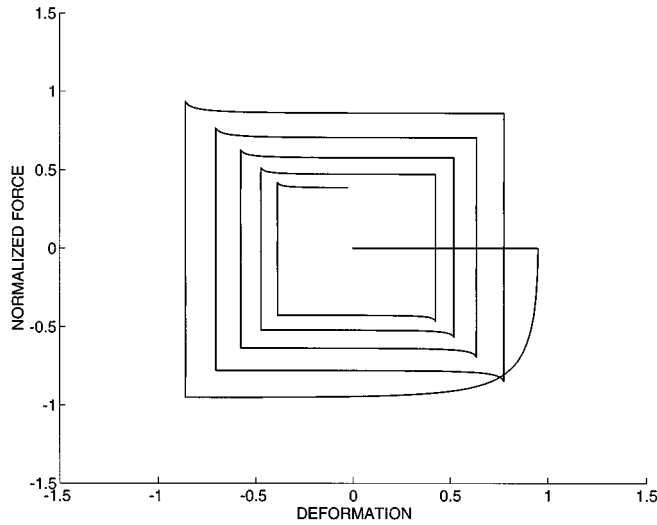


Figure 11. Effect of actuator dynamics in the hysteresis loop of a MHF dissipater

The resistance force of the dissipater is still expressed as

$$f(t) = \mu N(t) \operatorname{sgn} \left( \frac{d\Delta}{dt}(t) \right) \quad (52)$$

with  $N(t)$  given by the solution of equation (50). This non-linear model also gives an HD1 force–deformation relation, because if the deformation signal and the initial condition  $N_0$  are scaled by a constant, the force is scaled by the same constant.

Figure 11 shows the hysteresis loops of this model for the following parameters  $\tau_N = 0.05$  s,  $\mu = 0.20$  for  $\Delta(t) = \sin(2\pi t) e^{-0.2t}$ . The normalized force  $f(t)/g(\mu)$  is plotted as a function of the deformation  $\Delta(t)$ . This model is not rate-independent because of the actuator dynamics. However, for small actuator–response time to period of vibration ratios, the effect of actuator dynamics should not be significant.

## 6. EFFECT OF THE STIFFNESS OF THE MHF-DISSIPATER CONNECTOR

A dissipater is typically connected to a structural system with an elastic connector such as a diagonal brace, a Chevron bracing or some other flexible substructure. For this reason, a model of a semi-active friction damper should include some flexibility of the connecting members as shown at the top of Figure 12. In the figure,  $\Delta(t)$  is the deformation of the brace plus the deformation of the friction dissipater,  $f(t)$  the force in the dissipater and  $k_b$  the stiffness of the flexible connector.

If we let  $N(t)$  satisfy equation (50) with  $\Delta(t)$  the deformation of the friction damper plus the deformation of the elastic connector, the force in the MHF dissipater corresponds to the force in an elastoplastic element with variable yielding resistance. Therefore, the closed-loop system can be modelled as

$$f(t) = k_b(\Delta(t) - z(t)) \quad (53)$$

where the state variable  $z(t)$  is the zero-force deformation satisfies

$$\frac{dz(t)}{dt} = \frac{d\Delta(t)}{dt} \quad \text{if } |k_b(\Delta(t) - z(t))| = \mu N(t) \quad (54)$$

$$\frac{dz(t)}{dt} = 0 \quad \text{if } |k_b(\Delta(t) - z(t))| < \mu N(t) \quad (55)$$

with  $z(0) = 0$ .

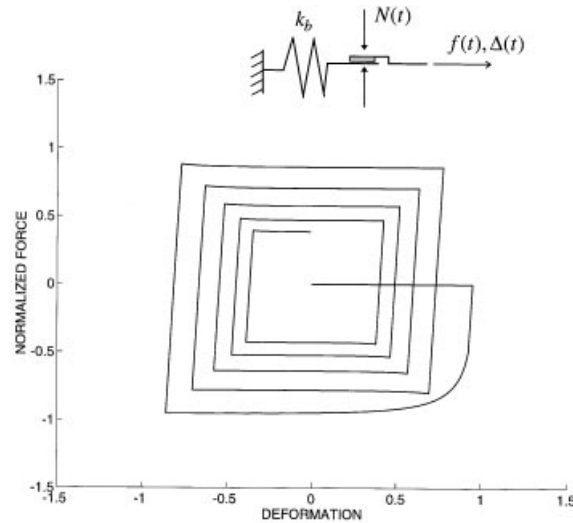


Figure 12. Schematic diagram of MHF dissipater with elastic connector and effect of connector flexibility and actuator dynamics on the hysteresis loop of the dissipater

It is not difficult to prove that if  $N(t)$  is given by equation (50), the force–deformation relation of the semi-active dissipater including connector flexibility (equations (50) and (53)) is HD1.

Figure 12 shows the hysteresis loops of a model of MHF dissipater including both actuator dynamics and flexibility of the connector. The parameters selected for the simulation were  $k_b/g = 1$ ,  $\mu = 0.10$ , and  $\tau_N = 0.05$  s. The deformation signal is  $\Delta(t) = \sin(2\pi t) e^{-0.2t}$ . The figure shows the normalized force  $f(t)/(\mu g)$  as a function of the deformation. The effects of both elasticity of the connector and actuator dynamics can be incorporated in this model providing a very powerful tool for the prediction of the response of structures with MHF dissipaters.

## 7. CONCLUDING COMMENTS

A new control algorithm for semi-active friction dissipaters has been proposed. The system is referred to as Modulated Homogeneous Friction (MHF). When operated with the proposed control logic, this semi-active friction dissipater shows a homogeneous-of-degree-one force–deformation relation. This non-linear constitutive relation shows very promising features such as quadratic dissipation of energy per cycle in the deformation amplitude, maximum dissipation efficiency for resistance-force level proportional to deformation, and simple and accurate linearization.

Some of the characteristics of structures incorporating this type of dissipater have been analysed including the free vibration response of SDOF structures, harmonic response of SDOF structures, and the existence of modes of vibration in the case of MDOF systems. The use of equivalent linear hysteretic elements to approximate the response of MDOF structures incorporating MHF dissipaters have proven very accurate.

A comparison of the performance of structures with this type of dissipater and structures with passive viscoelastic and frictional dissipaters should be conducted to assess the merits of this semi-active device. Experimental research should be conducted to verify the feasibility of the proposed semi-active device. This research should also confirm the need or not of further modelling techniques for the semi-active dissipater including aspects such as elasticity of the connectors, delays and dynamics of the actuator applying the desired contact force. The design of filters for the detection of local peaks in the deformation signal in the presence of noisy signals output by the sensors is another topic that requires investigation and experimental verification.

## ACKNOWLEDGEMENTS

This research was conducted with the financial support of the National Science Foundation under Grant No. BCS 9302101 and of the National Center for Earthquake Engineering Research of the University of New York at Buffalo. This support is greatly appreciated. The author thanks the reviewers for their valuable comments.

## REFERENCES

1. A. A. Ferri and B. S. Heck, 'Semi-active suspension using dry friction energy dissipation', *Proc. 1992 American control conf.*, Vol. 1, 1992, pp. 31–35.
2. D. Karnopp, M. J. Crosby and R. A. Harwood, 'Vibration control using semi-active force generators', *J. eng. ind. trans. ASME* **96**, 619–626 (1974).
3. D. Karnopp, 'Design principles for vibration control systems using semi-active dampers', *J. dyn. systems measurement control trans. ASME* **112**, 448–455 (1990).
4. Z. Akbay and H. K. Aktan, 'Actively regulated friction slip braces', *Proc. 6th Canadian conf. on earthquake engineering*, University of Toronto Press, Toronto, 1991.
5. Z. Akbay and H. M. Aktan, 'Intelligent energy dissipation devices', *Proc. 4th U.S. national conf. on earthquake engineering*, Palm Springs, Vol. 3, Earthquake Engineering Research Institute, 1990, pp. 427–435.
6. D. J. Dowdell and S. Cherry, 'Semi-active friction dampers for seismic response control of structures', *Proc. 5th U.S. national conf. on earthquake engineering*, Vol. I, Earthquake Engineering Research Institute, California, 1994, pp. 819–828.
7. T. Fujita, M. Shimazaki, Y. Hayamizu, S. Aizawa, M. Higashino and N. Haniuda, 'Semiactive seismic isolation using controllable friction damper', *Bull. earthquake resistant structure research center* (27) 21–31 (1994).
8. J. C. Hayen and W. D. Iwan, 'Response control of structural systems using active interface damping', in G. W. Housner, S. F. Masri and A. G. Chassiakos (eds), *Proc. 1st world conf. on structural control*, Vol. 1, University of Southern California, Los Angeles, 1994, pp. WA2/23–32.
9. K. Kawashima, S. Unjoh and H. Mukai, 'Seismic response control of highway bridges by variable damper', *Proc. 5th U.S. national conf. on earthquake engineering*, Vol. I, Earthquake Engineering Research Institute, California, 1994, pp. 829–838.
10. S. Kawamura, M. Shinozuka, S. Fujii and Q. Feng, 'Hybrid isolation system using friction-controllable sliding bearings', in Y. K. Wen (ed.), *Proc. int. workshop on intelligent systems, intelligent structures*, Vol. 2, monitoring and control, Elsevier Applied Science, London and New York, 1992.
11. S. Nagarajaiah, M. Q. Feng and M. Shinozuka, 'Control of structures with friction controllable sliding isolation bearings', *Soil dyn. earthquake eng.* **12** 103–112 (1993).
12. C. Yang and L. W. Lu, 'Seismic response control of cable-stayed bridges by semi-active friction damping', *Proc. U.S. national conf. on earthquake engineering*, Chicago, Vol. I, Earthquake Engineering Research Institute, 1994, pp. 911–920.
13. Z. Akbay and H. M. Aktan, 'Abating earthquake effects on buildings by active slip brace devices', *Shock vibr.* **2**, 133–142 (1995).
14. J. A. Inaudi and J. M. Kelly, 'Nonlinear homogeneous dynamical systems', *Report No. UCB/EEERC-93/11*, Earthquake Engineering Research, University of California at Berkeley, 1995.
15. S. Kannan, H. M. Uras and H. M. Aktan, 'Active control of building seismic response by energy dissipation', *Earthquake eng. struct. dyn.* **24**, 747–759 (1995).
16. T. K. Caughey and Vijayaraghavan, 'Free and forced oscillations of a dynamic system with linear hysteretic damping (nonlinear theory)', *Int. j. non-linear mech.* **5**, 533–555 (1970).
17. J. A. Inaudi, D. K. Nims and J. M. Kelly, 'On the analysis of structures with energy dissipating restraints', *Report No. UCB/EEERC-93/13*, Earthquake Engineering Research, University of California at Berkeley, 1993.
18. J. A. Inaudi, A. Zambrano and J. M. Kelly, 'On the analysis of structures with viscoelastic dampers', *Report No. UCB/EEERC-93/06*, Earthquake Engineering Research, University of California at Berkeley, 1993.
19. S. Cherry, 'Research on friction damping at the University of British Columbia', in Masri and Housner (eds) *Proc. int. workshop on structural control*, USC Publication No. CE-9311, University of Southern California, 1993, pp. 84–91.
20. M. Q. Feng, M. Shinozuka and S. Fujii, 'Friction-controllable sliding isolation system', *J. eng. mech. ASCE* **119**, 1845–1864 (1993).
21. J. A. Inaudi and J. Hayen, 'Research on variable-structure control in the United States', *Proc. post-smirt seminar on seismic isolation, passive energy dissipation and control of vibrations of structures*, University of Chile, Santiago, Chile, 1995.
22. J. A. Inaudi and J. M. Kelly, 'Dynamics of homogeneous frictional systems', in Vol I., A. Guran, F. Pfeiffer and K. Popp (eds.), *Dynamics with Friction: Modelling, Analysis and Experiments*, World Scientific, Singapore, 1995.
23. Z. Liang, M. Tong and G. C. Lee, 'Real-time structural parameter modification (RSPM): development of innervated structures', *Technical Report NCEER-95-0012*, National Center for Earthquake Engineering Research, University of New York at Buffalo, 1995.
24. W. H. Patten, Q. He, C. C. Kuo, L. Liu and R. L. Sack, 'Suppression of vehicle induced bridge vibration via semi-active hydraulic dampers (SAVD)', in G. W. Housner, S. F. Masri and A. G. Chassiakos (eds.), *Proc. 1st world conf. on structural control*, Vol. 3, University of Southern California, Los Angeles, 1994, pp. FA1/30–38.